HHS Public Access

Author manuscript

Depress Anxiety. Author manuscript; available in PMC 2018 January 01.

Published in final edited form as:

Depress Anxiety. 2017 January ; 34(1): 68–78. doi:10.1002/da.22549.

Decrease in Somatostatin-Positive Cell Density in the Amygdala of Females with Major Depression

Gaelle Douillard-Guilloux[1], **David Lewis**[1,2], **Marianne L. Seney**[1,§], and **Etienne Sibille**[1,2,3,§]

[1]Department of Psychiatry, University of Pittsburgh Medical School, Pittsburgh, PA, USA

[2]Center for Neuroscience, University of Pittsburgh, Pittsburgh, PA, USA

[3]Campbell Family Mental Health Research Institute of CAMH; Departments of Psychiatry, and of Pharmacology and Toxicology, University of Toronto, Toronto, CA

Abstract

Background—Somatostatin (SST) is a neuropeptide expressed in a subtype of gamma-aminobutyric acid (GABA) interneurons that target the dendrites of pyramidal neurons. We previously reported reduced levels of SST gene and protein expression in the postmortem amygdala of subjects with major depressive disorder (MDD). This reduction was specific to female subjects with MDD.

Methods—Here, we used in situ hybridization to examine the regional and cellular patterns of reductions in SST expression in a cohort of female MDD subjects with known SST deficits in the amygdala (N = 10/group).

Results—We report a significant reduction in the density of SST-labeled neurons in the lateral, basolateral, and basomedial nuclei of the amygdala of MDD subjects compared to controls. SST mRNA levels per neuron did not differ between MDD and control subjects in the lateral or basolateral nuclei, but were lower in the basomedial nucleus. There was no difference in cross-sectional density of total cells.

Conclusions—In summary, we report an MDD-related reduction in the density of detectable SST-positive neurons across several nuclei in the amygdala, with a reduction in SST mRNA per cell restricted to the basomedial nucleus. In the absence of changes in total cell density, these results suggest the possibility of a change in SST cell phenotype rather than cell death in the amygdala of female MDD subjects.

Keywords

Biological markers; Depression; Gender; Mood disorders; Genetics

[§]Corresponding authors: Marianne L. Seney, 450 Technology Drive, Bridgeside Point II Room 226, Pittsburgh, PA 15219, Phone: 412-624-3072; Fax: 412-624-5280, seneyml@upmc.edu; Etienne Sibille, 250 College Street, Toronto, ON M5T 1R8, Phone: 416-535-8501, ext 36571, Etienne.sibille@camh.ca.

CONFLICT OF INTEREST:

Douillard-Guilloux, Seney, and Sibille have no conflicts to disclose.

INTRODUCTION

Somatostatin (SST) is a neuromodulatory peptide expressed in a subtype of GABA neurons that specifically inhibit the dendritic compartment of excitatory pyramidal neurons[1]. Reduced SST expression has consistently been reported across several psychiatric [e.g.[2–9]] and neurodegenerative brain disorders [e.g.[10–12]]. We previously reported reduced SST gene expression in major depressive disorder (MDD). This pattern of reduced SST gene expression in MDD was found across several corticolimbic brain regions, including the dorsolateral prefrontal cortex[9], the subgenual anterior cingulate cortex (sgACC)[8] and the lateral and basomedial nuclei of the amygdala[13]. There was a sex difference in our findings that mimics the female vulnerability to MDD. Specifically, we found more robust SST reduction in female subjects in the sgACC[14] and a reduction only in females in the amygdala[13] [see[15] for no change in SST expression in the amygdala of male MDD subjects].

SST cells represent ~18–20% of interneurons and exhibit a laminar-specific pattern of expression in the cortex[16–18]. However, there is no laminar organization in the lateral and basolateral nuclei of the amygdala, and SST cells are uniformly distributed[19]. Within the basolateral amygdala, most SST cells display stuttering properties[20], similar to SST cells in layer 4 of the cortex[21]. As observed in the cortex, basolateral amygdala SST cells predominantly innervate the distal dendrites of excitatory pyramidal cells. Additionally, a small percentage of SST cells innervate other interneurons[19]. Interestingly, recent work has identified a novel subpopulation of basolateral amygdala SST cells that send long-range projections to the basal forebrain[22], although the electrophysiological properties and function of these long-range targeting cells remain unknown.

Here, we used in situ hybridization to quantify SST mRNA levels in the amygdala of MDD subjects for which we had a priori information of reduced SST expression, as measured by gene array and quantitative PCR in combined gray matter samples[8, 13]. Identifying whether the SST reduction is based on reduced SST per cell or reduced density of SST-positive cells has implications for mechanisms of disease and for therapeutic approaches. Thus, we characterized the specificity of the reduced SST in the lateral, basolateral and basomedial nuclei of the amygdala using measurements of the amount of SST expression per SST-positive cell and density of SST-positive cells in each amygdala region.

MATERIAL AND METHODS

Human postmortem subjects

Brain samples were obtained after consent was provided by next of kin during autopsies conducted at the Allegheny County Medical Examiner's Office (Pittsburgh, USA). The University of Pittsburgh's Institutional Review Board and Committee for Oversight of Research Involving the Dead approved all procedures. An independent committee of experienced clinical research scientists made consensus DSM-IV diagnoses for each subject using structured interviews with family members as well as review of medical records and toxicology results; the absence of psychiatric diagnoses was confirmed in control subjects using the same approach[23].

A cohort of 10 subject pairs was created consisting of female subjects with MDD and female control subjects. To control for biological and experimental variance, subjects with MDD were matched to comparison subjects for race and as closely as possible for age. All selected brains were analyzed for adequate brain pH (> 6.4) and RNA integrity by optical density (OD ≥ 1.6) and Agilent bioanalyzer analysis (Agilent Technologies, Palo Alto, CA; RIN expert scoring system ≥ 7) as previously described[15]. Subject groups did not differ in mean age, postmortem interval (PMI), RNA integrity number (RIN), and RNA ratio ($p>0.05$). There was a significant effect of group on brain pH, which we accounted for by using pH as a covariate in our statistical model (see statistical analysis). Subjects were selected for rapid modes of death and short agonal phases to limit the effect of these factors on RNA quality and pH[24], while subjects with advanced disease stages (i.e., cancer, neurodegenerative disorders) were excluded. This cohort is a subset of a larger cohort used previously, and subjects were selected to enrich the cohort in MDD subjects with robust reduction in SST expression[13] since the aim of this study was not to confirm the reduction of SST in MDD, but rather to further determine the nature of the reduction (i.e., whether the reduction is specific to a particular nucleus of the amygdala, whether there is loss of SST-positive cells or reduction in SST per cell).

In situ hybridization

Templates for the synthesis of the antisense and sense riboprobes were generated by PCR using specific primers to amplify a 337 base pair fragment of human SST. These fragments corresponded to bases 112–448 of the human SST gene (GenBank NM_001048). ^{35}S-labeled riboprobes were generated by in vitro transcription and hybridized to two sections (separated by 140 μm) from each subject. In situ hybridization probes, methods, and analyses were performed as previously described[2, 13, 25]. Matched subjects were processed together to reduce experimental variance.

Each slide was randomly coded, such that subject number and diagnosis were unknown to the experimenter. Sections were trans-illuminated and brightfield photomicrographs were captured, digitized, and analyzed with Microcomputer Imaging Device (MCID; Imaging Research Inc., London, Ontario, Canada) software. The sections, as well as [^{14}C]-standards, were exposed on the same BioMax MR film (Kodak, Rochester, NY) for 3 days and analyzed using MCID.

Evaluation of mRNA expression at the cellular level was performed by determining silver grain accumulation on emulsion-dipped, Cresyl Violet counter-stained sections. After digitizing each autoradiographic film section, the in situ hybridized slides were coated with liquid emulsion at 43° (KODAK Autoradiography Emulsion, Type NTB for light Microscope Autoradiography). Slides were dipped for one minute using an automated dipping machine. Slides were then wrapped in aluminum foil in a plastic box and incubated at 4°C for 12 days. The coated slides were then dipped for 4 minutes in developer, 1 minute in Milli-Q water, and 8 minutes in fixer. Emulsion coated slides were counterstained immediately after being developed. Tissue sections were stained for 10 seconds with 0.5% Cresyl Violet solution, followed by two rinses in Milli-Q water. Slides were then dehydrated with a graded ethanol series, followed by xylene, and coverslipped with Permount.

Developed slides counterstained with cresyl violet were superimposed onto images captured before dipping (brightfield digitized image of the dried slides) to draw contours of each nucleus (lateral, basal and mediobasal nucleus) onto the dipped slides. Amygdala regions were then confirmed in adjacent sections stained for acetylcholinesterase and Nissl substance.

Sampling strategy for each amygdala nucleus

Using the MCID system coupled to a microscope equipped with a motor-driven stage, a region of interest (ROI) (Figure 1B–C) was defined for each nucleus by a square including the nucleus. Since these amygdala nuclei are irregular in shape, the ROI squares were placed such that each irregularly shaped nucleus fell within its respective ROI square (see Figure 1). Three traverses (from the dorsal surface to the ventral surface) were placed in each ROI and two sections were analyzed per subject (separated by 140 μm). For the lateral nucleus, the lateral traverse (LT) was drawn at 20% of the distance from the lateral to the medial border, the medial traverse (MT) at 50%, and the central traverse (CT) at 90%. For the basolateral nucleus, the LT was drawn at 20%, the MT at 30%, and the CT at 70% of the distance from the lateral to the medial border of the nuclei. Ten sampling frames (500μm × 500μm) were placed in each of the three traverses (for a total of 30 sampling frames per nucleus) from 10% to 90% from the dorsal to ventral surface (Figure 1B–C). Due to the relatively smaller size of the basomedial nucleus, bins were placed to cover the entire nucleus, from 10% to 90% of the distance from the lateral to the medial border and from 10% to 90% from the dorsal to the ventral border of this ROI.

Density of SST positive cell clusters and expression of SST mRNA per cluster

Since RNase A treatment during the in situ hybridization procedure degrades Nissl-stainable substances within the cytoplasm, it was not possible to draw contours around the soma of neurons. Thus, we used the pattern of grain clusters to identify SST-positive cells. We divided the SST-positive neurons into three major categories [types 1 (small spherical), 2 (large multipolar), and 3 (fusiform); as in[26]]. Within each cell type, there was some heterogeneity with regard to the soma size and the number and caliber of the dendrites. The majority of neurons fit into the type I category (small and spherical), ranging in diameter from approximately 8 to 20μm. We also found very dense and spread-out grain clusters in each nucleus of the amygdala that were much larger than a 20μm diameter circle (See main text and Figure 2); these clusters seemed to represent more than one SST cell in close proximity. Accordingly, we analyzed the density of small SST clusters per mm^2 (i.e., single SST positive cells) as well as the density of large clusters per mm^2 (i.e., large SST positive cell or multiple SST positive cells in close proximity). Within each bin, we used a circle with a fixed diameter of 15μm (177 μm^2; within the size range of type I cells) for the small clusters or 25μm (491 μm^2; larger than the size of a single type I cell) for the large clusters. Using these two circle sizes, we measured: 1) cluster density per mm^2 (we use cluster density as a proxy measure of the number of SST cells) and 2) the ratio of circle covered by grains (we use this as a measure of SST expression per SST-positive cell). Compared to the small clusters, large clusters showed considerable grain overlap and higher signal intensity, making it more difficult to count the number of individual grains in large clusters. Due to the difference in SST expression between small and large clusters, there was no appropriate

exposure time that would be able to capture both the small and large clusters under optimal conditions (since this is emulsion-dipped and not film-based). Thus, we used a single exposure time to detect both small and large clusters, and instead used the ratio of area covered by grains within each circle as a proxy measure of amount of SST per positive cell (both small and large). For each darkfield slide section, background noise was first minimized (similarly across all analyzed sections). After background minimization, MCID imaging software was used to calculate the ratio of area covered by grains within each sampling circle placed over grain clusters[2]. In other words, the 15μm or 25μm circles were placed over clusters and the "ratio" consisted of the pixels within the circle covered by grain clusters divided by the pixels within the circle not containing grain clusters. Background grain count measures were sampled from circles placed over all cell clusters in a region of the white matter. Thus, these analyses gave us estimates of the density of SST positive cells per mm^2 and the level of SST expression per SST positive cell (ratio of area covered by grains) in each amygdala nucleus. We also determined the density of cresyl violet stained cells per mm^2 within each amygdala region as a proxy measure for number of cells within each nucleus.

Statistical analysis

To determine relevant scale covariates to include in the analysis of covariance (ANCOVA) model, Pearson correlation was used to assess the effect of age, postmortem interval, brain pH, and RNA integrity (RIN) on in situ hybridization measures. To determine relevant categorical covariates (alcohol abuse, antidepressant use, death by suicide), in situ hybridization measurements were tested by analysis of variance (ANOVA); note that only MDD subjects were used to assess potential effects of antidepressant use, death by suicide, and alcohol use. See Supplementary Tables 1 and 2 for details on statistics associated with covariate testing. The modified Bonferroni-Holm method was used to correct for testing of multiple covariates. pH was the most consistent covariate used in the ANCOVA models, as pH is significantly higher in MDD compared to control ($p < 0.001$). Uncorrected ANCOVA p-values are reported for the analyses comparing in situ hybridization measures in controls versus MDD subjects, as we have a priori information of reduced tissue level SST expression in MDD in these same subjects.

RESULTS

We previously reported significantly reduced SST expression in MDD by qPCR and Western Blotting in the basolateral complex of the amygdala and by in situ hybridization in the lateral and basomedial nuclei of the amygdala[13]. In order to determine if all or a subset of SST neurons were affected in the lateral, basolateral, and basomedial nuclei of the basolateral complex of the amygdala, we determined 1) the density of SST positive cells in each amygdala nucleus and 2) the SST mRNA levels per neuron by assessing the ratio of the area covered by silver grains in SST silver grain clusters.

MDD subjects have lower density of detectable SST positive cells in the amygdala

We found a general reduction in the density of SST positive clusters in MDD subjects in all three nuclei of the amygdala examined (lateral, basolateral, basomedial). Specifically, there

was a 41% reduction in the density of SST positive clusters (small and large clusters combined) in the lateral nucleus ($p = 0.001$), a 45% reduction in the basolateral nucleus ($p < 0.001$), and a 52% reduction in the basomedial nucleus ($p < 0.001$) of MDD subjects compared to controls (Figure 3A). This same pattern was found when the analysis was split by cluster size. There was a 34% reduction in the density of large clusters ($p < 0.02$) and a 47% reduction in the density of small clusters ($p < 0.005$) in the lateral nucleus in MDD subjects. In the basolateral nucleus, there was a 40% reduction in the density of large clusters ($p < 0.01$) and a 43% reduction in the density of small clusters ($p < 0.002$) in MDD subjects. Similarly, there was a 40% reduction in density of large clusters ($p < 0.004$) and a 47% reduction in density of small clusters ($p < 0.004$) in the basomedial nucleus in MDD subjects. In parallel, we found no significant reduction in the density of cresyl violet stained cell bodies (both SST-positive and SST-negative combined; see Supplementary Figure 1).

MDD subjects have reduced SST mRNA per cell only in the basomedial nucleus of the amygdala

As a measure of the expression of SST per SST-positive cell, we calculated the ratio of the area covered by silver grains for the small and large clusters. In the basomedial nucleus, there was a 25% reduction in the ratio of area covered by silver grains per cluster (small and large clusters combined) in MDD subjects compared to controls ($p < 0.04$; Figure 3B). We found this same result when we split the analysis by cluster size. Specifically, the ratio of the area covered by silver grains per cluster was reduced by 20% in large clusters ($p < 0.04$) and by 32% in small clusters ($p < 0.01$) in MDD subjects compared to controls. MDD subjects and controls did not differ in the ratio of area covered by silver grains per cluster in the lateral nucleus (all clusters: $p > 0.3$; large clusters: $p > 0.25$; small clusters: $p > 0.15$) or in the basolateral nucleus (all clusters: $p > 0.4$; large clusters: $p > 0.1$; small clusters: $p > 0.85$) (Figure 3B).

DISCUSSION

Reduced SST in MDD across corticolimbic brain regions

In addition to reduced SST expression in the amygdala of MDD subjects (as reported here and in[13]), we previously showed that SST expression is reduced in other corticolimbic brain regions in subjects with MDD, namely the subgenual anterior cingulate cortex (sgACC[8, 25]) and dorsolateral prefrontal cortex (DLPFC[14]). Thus, the reduced SST in MDD subjects appears to be a general finding as opposed to specific to the amygdala. Whether SST is reduced in additional corticolimbic or other brain regions of patients with MDD (e.g. the hippocampus) is unknown. We have used a strategy similar to the one used in the current study to examine the specificity of reduced SST in the sgACC of subjects with MDD. In contrast to the results presented here in the amygdala, we reported a robust reduction in SST mRNA expression per cell across cortical layers, and surprisingly no change in the density of SST-positive cells in the sgACC in subjects with MDD[25]. Thus, the reduced tissue-level SST expression may occur through different mechanisms across corticolimbic brain regions. Using preclinical chronic stress models in mice, we showed that SST cells are selectively vulnerable to biological adversity, specifically affecting proteostasis, also known as endoplasmic reticulum (ER) stress[27]. The outcome of such an event is reduced expression of

non-essential genes, leading to cell death in somatic tissue and to loss of cellular phenotype in non-dividing neurons[28]. If applicable to human subjects, it is conceivable that the results in the amygdala represent a more severe phenotype compared to the sgACC. For instance, we may be seeing a reduced density of SST-positive cells in the amygdala due to an ER stress-induced profound reduction in the amount of SST per cell, putting these cells below our level of detection as SST-positive. However the lack of a gradient effect (i.e., intermediate and progressive loss of SST expression per cell) suggests that other mechanisms may be at play. We previously showed in rodent models that the expression of SST and other GABA-related neurons are affected by sex-related factors, namely circulating hormones and XY-related genetic factors[14, 29], and consistent sex differences in gene expression are observed in the amygdala between mice and humans[30]. Moreover, we found that the reduced expression of SST was more robust in female compared to male subjects in the sgACC[14], and only female MDD subjects have reduced SST expression in the amygdala[13, 15]. Together this suggests that sex-related factors may mediate the SST cellular pathology in MDD, a hypothesis that is of great interest, in view of the increased vulnerability of women to develop MDD[31, 32].

Effects of reduced SST on local and amygdala circuitry

We previously found that SST expression is significantly decreased in the lateral and the basomedial nuclei in female MDD subjects compared to controls[13]. The lateral nucleus receives major input from the sensory cortex and the sensory thalamus and sends heavy projections to most other amygdala nuclei[33]. Although relatively little is known about the amygdala cell circuit, the nuclei investigated present cortical-like organization (although not in a layered pattern), and incoming excitatory signals are similarly regulated by inhibitory interneurons, such as SST-positive interneurons. A decrease in feedback inhibition in the lateral nucleus of the amygdala due to reduced density of SST-positive cells would imply impaired excitation/inhibition balance for all amygdala nuclei that receive projections from the lateral nucleus. In this study, we only examined SST expression. Thus, it is unclear whether there is a reduction in inhibitory GABA signaling in these amygdala nuclei as well. However, in our previous study comparing gene expression in the amygdala of female MDD subjects and controls[13], we observed a reduction in several GABA-related transcripts, including the GABA synthesizing enzyme, glutamate decarboxylase 1 (GAD1), and the GABA receptor subunit, GABRA1; this suggests that there may indeed be reduced inhibition in these amygdala nuclei in female MDD subjects. Future studies may follow-up by using in situ hybridization for GAD1 or GAD2 in MDD and control subjects to achieve more spatial resolution.

Specificity of reduced SST

Reduced SST expression has been reported across brain regions in MDD but also in schizophrenia[2], bipolar disorder[15], Alzheimer's disease[10], and during normal aging[34]. Low SST interacts in a complex biological landscape of additional interacting pathological modules with specific environmental factors and developmental trajectories for each of these disorders[13, 34]. At the cell and local circuit levels, the specific consequence of low SST will depend on: 1) whether all SST neurons are affected, 2) whether deficits extend to altered levels of co-expressed neuromodulatory peptides within those cell populations (i.e., is there

also decreased expression of neuropeptide Y and/or cortistatin?), 3) whether GABA function itself is affected (see above), and 4) the presence of additional pathologies or compensatory mechanisms in other cell types comprising the local canonical cell circuit, for instance parvalbumin (PV)- or vasoactive intestinal peptide (VIP)-positive GABA neurons and pyramidal cells.

The fact that the density of detectable SST-positive cells is reduced in the amygdala is a first step to understanding the specificity of low SST in the amygdala in the context of MDD. This may reflect an early developmental effect or a selective vulnerability of those cells to environmental stress. We did not find a decrease in density of all cresyl violet stained cells (SST-positive combined with SST-negative), suggesting that either: 1) at the moment of death, the loss in SST-positive cells in the amygdala was compensated for by an increase of cells not expressing SST (e.g., reactive astrocytes), or 2) there was not a loss of cells, but rather a change in phenotype of these cells (e.g., these neurons no longer express SST). Hence, a reduction in the density of SST-positive cells in MDD subjects in the absence of change in total cell density could represent a developmental deficit in generating SST cells or a complete loss of SST expression per cell (or at least a loss of SST expression under our capacity of detection) without a loss of those cells. These hypotheses are not unique to MDD, as they have been suggested in schizophrenia, in which both SST cell density and SST expression per cell is reduced in the DLPFC[2]. It may be that reduced SST is both an early developmental pathological event and a later episodic event that synergizes with other pathological processes, resulting in the unique neuropsychiatric or neurological disorder.

Limitations

Some of the limitations of these results are inherent to the investigation of heterogeneous human psychiatric disease cohorts and of postmortem brain samples. Large numbers of clinical, demographic and technical parameters have to be taken into consideration, and results are mostly correlative and cannot provide insights into developmental processes in MDD. We used fairly stringent criteria for inclusion of covariates, only including those that survived after correction for multiple testing. Additionally, since we assessed effects of suicide and antidepressant use in only MDD subjects (10 subjects), this reduced the probability of detecting differences. Our smaller cohort size was chosen to evaluate the specificity of SST reduction, and was not powered to evaluate relevant modulators such as age[8].

CONCLUSION

Here, we used postmortem brain samples from female MDD subjects with known reductions in amygdala SST expression at the gene and protein level to characterize whether there was a reduction in the density of SST positive neurons and/or a reduction of SST mRNA expression per neuron. Of note, we only examined females here, as male MDD subjects showed no change in SST mRNA[15]. Results demonstrate a general reduction in the density of detectable SST-positive neurons in the lateral, basolateral, and basomedial nuclei, whereas a reduction in SST mRNA per neuron was only detected in the basomedial nucleus of the amgydala in MDD subjects. The relative density of all cells in each amygdala region did not

differ between MDD and control subjects. Together this suggests a potential change (or loss) in SST cell phenotype in MDD subjects rather than fewer SST-positive neurons.

Supplementary Material

Refer to Web version on PubMed Central for supplementary material.

Acknowledgments

This work was supported by National Institute of Mental Health (NIMH) MH084060 (ES), MH085111 (ES), and MH103473 (MS). The funding agency had no role in the study design, data collection and analysis, decision to publish and preparation of the manuscript. The content is solely the responsibility of the authors and does not necessarily represent the official views of the NIMH or the National Institutes of Health.

David A. Lewis currently receives investigator-initiated research support from Pfizer. In 2013–2015, he served as a consultant in the areas of target identification and validation and new compound development to Autifony, Bristol-Myers Squibb, Concert Pharmaceuticals and Sunovion.

References

1. Viollet C, Lepousez G, Loudes C, Videau C, et al. Somatostatinergic systems in brain: networks and functions. Molecular and cellular endocrinology. 2008; 286(1–2):75–87. [PubMed: 17997029]
2. Morris HM, Hashimoto T, Lewis DA. Alterations in somatostatin mRNA expression in the dorsolateral prefrontal cortex of subjects with schizophrenia or schizoaffective disorder. Cereb Cortex. 2008; 18(7):1575–87. [PubMed: 18203698]
3. Bissette G, Widerlov E, Walleus H, Karlsson I, et al. Alterations in cerebrospinal fluid concentrations of somatostatinlike immunoreactivity in neuropsychiatric disorders. Archives of general psychiatry. 1986; 43(12):1148–51. [PubMed: 3778111]
4. Konradi C, Zimmerman EI, Yang CK, Lohmann KM, et al. Hippocampal Interneurons in Bipolar Disorder. Arch Gen Psychiatry. 2010
5. Agren H, Lundqvist G. Low levels of somatostatin in human CSF mark depressive episodes. Psychoneuroendocrinology. 1984; 9(3):233–48. [PubMed: 6149588]
6. Kling MA, Rubinow DR, Doran AR, Roy A, et al. Cerebrospinal fluid immunoreactive somatostatin concentrations in patients with Cushing's disease and major depression: relationship to indices of corticotropin-releasing hormone and cortisol secretion. Neuroendocrinology. 1993; 57(1):79–88. [PubMed: 8097579]
7. Molchan SE, Hill JL, Martinez RA, Lawlor BA, et al. CSF somatostatin in Alzheimer's disease and major depression: relationship to hypothalamic-pituitary-adrenal axis and clinical measures. Psychoneuroendocrinology. 1993; 18(7):509–19. [PubMed: 7903467]
8. Tripp A, Kota RS, Lewis DA, Sibille E. Reduced somatostatin in subgenual anterior cingulate cortex in major depression. Neurobiology of disease. 2011; 42(1):116–24. [PubMed: 21232602]
9. Sibille E, Morris HM, Kota RS, Lewis DA. GABA-related transcripts in the dorsolateral prefrontal cortex in mood disorders. Int J Neuropsychopharmacol. 2011; 14(6):721–34. [PubMed: 21226980]
10. Gahete MD, Rubio A, Duran-Prado M, Avila J, et al. Expression of Somatostatin, cortistatin, and their receptors, as well as dopamine receptors, but not of neprilysin, are reduced in the temporal lobe of Alzheimer's disease patients. J Alzheimers Dis. 2010; 20(2):465–75. [PubMed: 20164562]
11. Davies P, Terry RD. Cortical somatostatin-like immunoreactivity in cases of Alzheimer's disease and senile dementia of the Alzheimer type. Neurobiol Aging. 1981; 2(1):9–14. [PubMed: 6115327]
12. Dupont E, Christensen SE, Hansen AP, de Fine Olivarius B, et al. Low cerebrospinal fluid somatostatin in Parkinson disease: an irreversible abnormality. Neurology. 1982; 32(3):312–4. [PubMed: 6121303]

13. Guilloux JP, Douillard-Guilloux G, Kota R, Wang X, et al. Molecular evidence for BDNF- and GABA-related dysfunctions in the amygdala of female subjects with major depression. Molecular psychiatry. 2012; 17(11):1130–42. [PubMed: 21912391]
14. Seney ML, Chang LC, Oh H, Wang X, et al. The Role of Genetic Sex in Affect Regulation and Expression of GABA-Related Genes Across Species. Frontiers in psychiatry. 2013; 4:104. [PubMed: 24062698]
15. Sibille E, Wang Y, Joeyen-Waldorf J, Gaiteri C, et al. A molecular signature of depression in the amygdala. The American journal of psychiatry. 2009; 166(9):1011–24. [PubMed: 19605536]
16. Lewis DA, Campbell MJ, Morrison JH. An immunohistochemical characterization of somatostatin-28 and somatostatin-281-12 in monkey prefrontal cortex. J Comp Neurol. 1986; 248(1):1–18. [PubMed: 2873154]
17. McDonald AJ, Mascagni F. Immunohistochemical characterization of somatostatin containing interneurons in the rat basolateral amygdala. Brain Res. 2002; 943(2):237–44. [PubMed: 12101046]
18. Weckbecker G, Lewis I, Albert R, Schmid HA, et al. Opportunities in somatostatin research: biological, chemical and therapeutic aspects. Nat Rev Drug Discov. 2003; 2(12):999–1017. [PubMed: 14654798]
19. Muller JF, Mascagni F, McDonald AJ. Postsynaptic targets of somatostatin-containing interneurons in the rat basolateral amygdala. J Comp Neurol. 2007; 500(3):513–29. [PubMed: 17120289]
20. Sosulina L, Graebenitz S, Pape HC. GABAergic interneurons in the mouse lateral amygdala: a classification study. J Neurophysiol. 2010; 104(2):617–26. [PubMed: 20484532]
21. Ma Y, Hu H, Berrebi AS, Mathers PH, et al. Distinct subtypes of somatostatin-containing neocortical interneurons revealed in transgenic mice. J Neurosci. 2006; 26(19):5069–82. [PubMed: 16687498]
22. McDonald AJ, Mascagni F, Zaric V. Subpopulations of somatostatin-immunoreactive non-pyramidal neurons in the amygdala and adjacent external capsule project to the basal forebrain: evidence for the existence of GABAergic projection neurons in the cortical nuclei and basolateral nuclear complex. Front Neural Circuits. 2012; 6:46. [PubMed: 22837739]
23. Glantz LA, Austin MC, Lewis DA. Normal cellular levels of synaptophysin mRNA expression in the prefrontal cortex of subjects with schizophrenia. Biol Psychiatry. 2000; 48(5):389–97. [PubMed: 10978722]
24. Beneyto, M.; Sibille, E.; Lewis, DA. Human postmortem brain research in mental illness syndromes. In: Charney, DS.; Nestler, EJ., editors. Neurobiology of Mental Illness. New York: Oxford University Press; 2008. p. 202-14.
25. Seney ML, Tripp A, McCune S, D AL, et al. Laminar and cellular analyses of reduced somatostatin gene expression in the subgenual anterior cingulate cortex in major depression. Neurobiology of disease. 2015; 73:213–9. [PubMed: 25315685]
26. Sorvari H, Soininen H, Paljarvi L, Karkola K, et al. Distribution of parvalbumin-immunoreactive cells and fibers in the human amygdaloid complex. J Comp Neurol. 1995; 360(2):185–212. [PubMed: 8522643]
27. Lin LC, Sibille E. Somatostatin, neuronal vulnerability and behavioral emotionality. Molecular psychiatry. 2015; 20(3):377–87. [PubMed: 25600109]
28. Roussel BD, Kruppa AJ, Miranda E, Crowther DC, et al. Endoplasmic reticulum dysfunction in neurological disease. Lancet Neurol. 2013; 12(1):105–18. [PubMed: 23237905]
29. Seney ML, Ekong KI, Ding Y, Tseng GC, et al. Sex chromosome complement regulates expression of mood-related genes. Biology of sex differences. 2013; 4(1):20. [PubMed: 24199867]
30. Lin LC, Lewis DA, Sibille E. A human-mouse conserved sex bias in amygdala gene expression related to circadian clock and energy metabolism. Mol Brain. 2011; 4:18. [PubMed: 21542937]
31. Kornstein SG, Schatzberg AF, Thase ME, Yonkers KA, et al. Gender differences in treatment response to sertraline versus imipramine in chronic depression. The American journal of psychiatry. 2000; 157(9):1445–52. [PubMed: 10964861]
32. Kessler RC, Berglund P, Demler O, Jin R, et al. Lifetime prevalence and age-of-onset distributions of DSM-IV disorders in the National Comorbidity Survey Replication. Archives of general psychiatry. 2005; 62(6):593–602. [PubMed: 15939837]

33. Pitkanen A, Savander V, LeDoux JE. Organization of intra-amygdaloid circuitries in the rat: an emerging framework for understanding functions of the amygdala. Trends in neurosciences. 1997; 20(11):517–23. [PubMed: 9364666]

34. Glorioso C, Oh S, Douillard GG, Sibille E. Brain molecular aging, promotion of neurological disease and modulation by Sirtuin5 longevity gene polymorphism. Neurobiol Dis. 2011; 41(2): 279–90. [PubMed: 20887790]

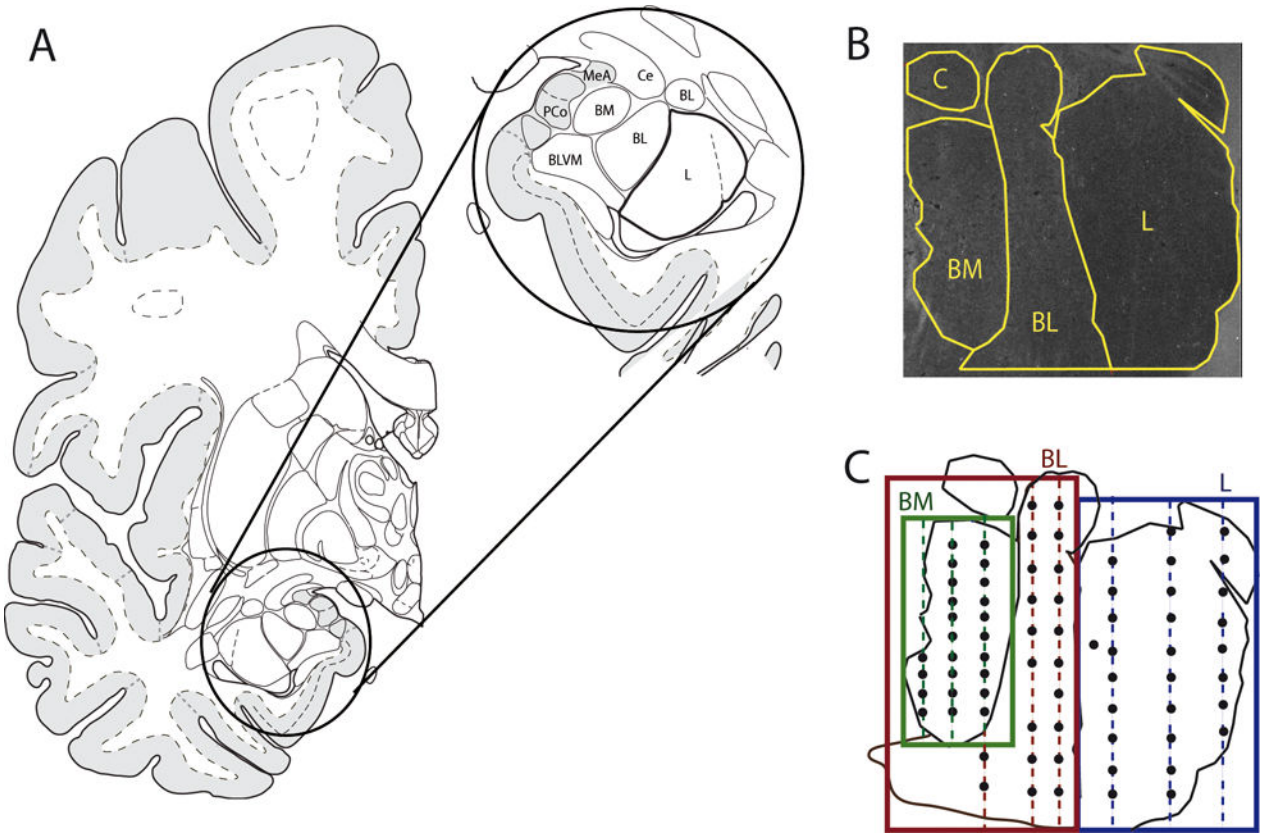

Figure 1. Sampling strategy in amygdala

(A) Diagram indicating lateral (L), basolateral (BL), and basomedial (BM) amygdala details. Offset circle on right is magnification of diagram on the left. (B) Dark field image of amygdala section with representation of L, BL, and BM nuclei. (D). Schematic representation of the sampling strategy in the amygdala. For the BL and L nuclei, three traverses from the dorsal surface to the ventral surface (lateral traverse; medial traverse; central traverse) where placed in each region of interest. Ten sampling bins were placed in each traverse from 10% to 90% from the dorsal to the ventral surface of the traverse. Due to the relatively smaller size of the BM nucleus, bins were placed to cover the entire nucleus, from 10% to 90% of the distance from the lateral to the medial border and from 10% to 90% from the dorsal to the ventral border of this nucleus.

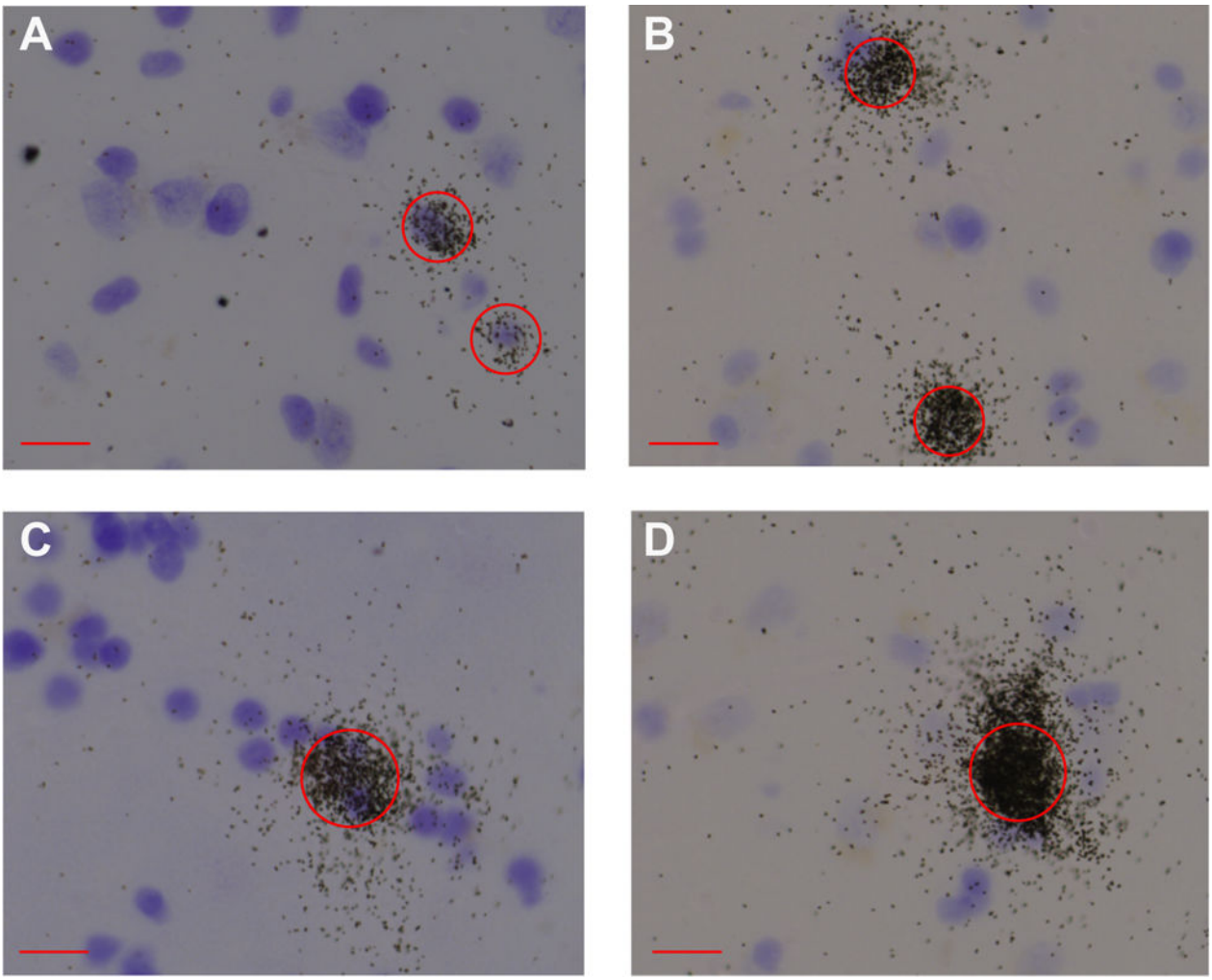

Figure 2. Patterns of SST-positive grain clusters in amygdala

Circles with a 15μm diameter (A–B) or 25μm (C–D) were centered over SST-positive nuclei. Circles were centered over SST-positive nuclei and other neurons in every counting frame, and the ratio of area covered by silver grains was calculated in the corresponding darkfield image. Compared to the small clusters (A and B), large clusters (C and D) showed considerable grain overlap and higher signal intensity, making it more difficult to count the number of individual grains in large clusters. Thus, we instead used the ratio of area covered by grains within each circle as a proxy measure of amount of SST per positive cell (both small and large). Scale bar = 15μm.

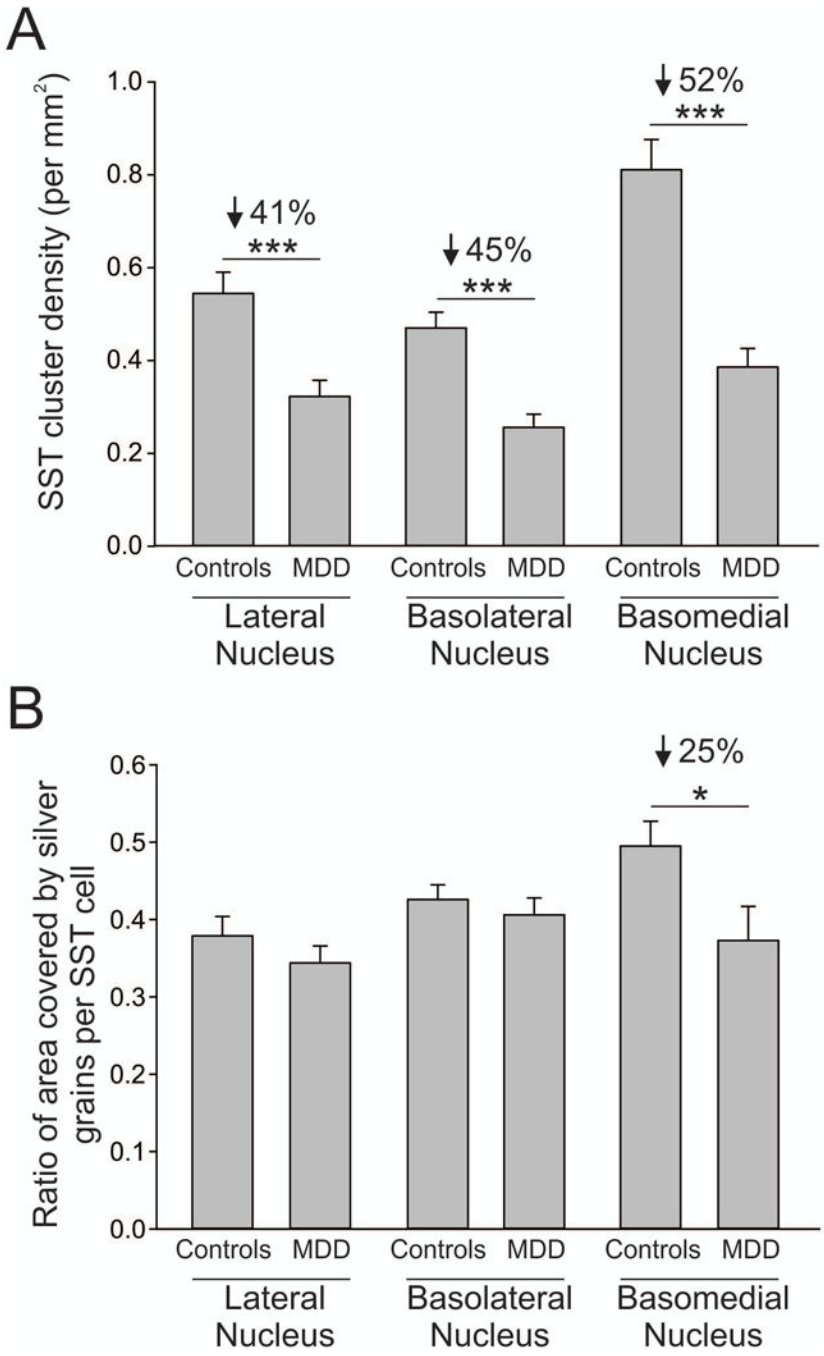

Figure 3. SST reduction in amygdala subregions of female MDD subjects

(A) MDD subjects have reduced SST cluster density in the lateral (−41%), basolateral (−45%), and basomedial (−52%) nuclei of the amygdala. (B) MDD subjects have reduced ratio of area covered by silver grains in only the basomedial nucleus (−25%) of the amygdala. Results are represented as mean +/− standard error of mean. ***, $p < 0.001$; *, $p < 0.05$.

Table 1

Subject characteristics.

Major Depression Group										Control Group							
Case	**Age**	**PMI**	**pH**	**RNA ratio**	**RIN**	**Suicide**	**AD ATOD**	**Alcohol ATOD**	**Cause of death**	**Case**	**Age**	**PMI**	**pH**	**RNA ratio**	**RIN**	**Alcohol ATOD**	**Cause of death**
1143	46	23.4	6.4	1.8	8.1	N	Y	Y	Drug overdose	686	52	22.6	7.1	1.9	8.5	N	ASCVD
1041	52	10.3	6.51	1.48	8.4	N	Y	Y	Drug overdose	1391	51	7.8	6.57	1.59	7.1	N	ASCVD
1190	47	22.3	6.55	1.64	8	Y	N	Y	Asphyxiation	567	46	15	6.77	2.26	8.9	N	Mitral valve prolapse
1221	28	24.8	6.61	1.83	7.2	N	N	N	Pulmonary thrombosis	546	37	23.5	6.74	1.95	8.6	N	ASCVD
1249	40	11.2	6.52	2.04	9	N	Y	N	Drug overdose	1092	40	16.6	6.83	1.68	8	N	Mitral valve prolapse
1271	50	18.6	6.35	1.82	8.6	N	Y	Y	Drug overdose	1318	58	18.8	6.69	1.95	7.4	N	ASCVD
1289	46	25	6.27	1.35	7.3	N	U	N	ASCVD	1280	50	23.5	6.65	1.33	7.7	N	Pulmonary thromboemboli
1332	46	17.5	6.49	1.6	8.9	N	Y	N	ASCVD	627	43	14.1	7.09	1	7	N	COPD
1356	60	20.6	6.06	1.78	8.5	N	Y	Y	Intraperitoneal hemorrhage	818	67	24	7.06	1.48	8.4	N	Anaphylactic reaction
1360	59	18.1	6.43	1.41	7.6	Y	Y	N	Drowning	1081	57	14.9	6.78	1.8	9	N	COPD
Mean	47.4	19.18	6.42	1.68	8.16						50.1	18.1	6.83	1.69	8.06		
SD	9.18	5.18	0.16	0.22	0.63						9.07	5.35	0.19	0.36	0.73		

Abbreviations: AD, antidepressants; ASCVD, arteriosclerotic cardiovascular disease; ATOD, at time of death; COPD, chronic obstructive pulmonary disease; MDD, major depressive disorder; PMI, postmortem interval in hours; RIN, RNA integrity number; SD, standard deviation.

Table 2

SST reduction by cluster density in the amygdala.

	All					Large clusters					Small Clusters				
	Control[1]	MDD[1]	%	F	p-value	Control[1]	MDD[1]	%	F	p-value	Control[1]	MDD[1]	%	F	p-value
Lateral nucleus															
Lateral traverse	0.460 (0.044)	0.259 (0.035)	−44	13.4	0.002	0.151 (0.019)	0.099 (0.019)	−35	3.85	0.065	0.324 (0.041)	0.190 (0.025)	−41	7.90	0.012
Medial traverse	0.506 (0.060)	0.310 (0.051)	−39	6.31	0.022	0.208 (0.032)	0.155 (0.025)	−25	1.65	0.215	0.314 (0.028)	0.171 (0.022)	−45	15.3	0.001
Central traverse	0.593 (0.057)	0.376 (0.047)	−37	8.95	0.008	0.253 (0.032)	0.171 (0.022)	−32	4.66	0.045	0.356 (0.035)	0.244 (0.032)	−31	5.30	0.034
Mean	0.545 (0.047)	0.323 (0.035)	−41	14.9	0.001	0.220 (0.25)	0.146 (0.013)	−34	7.05	0.016	0.458 (0.060)	0.243 (0.019)	−47	11.9	0.003
BasoLateral nucleus															
Lateral traverse	0.429 (0.054)	0.238 (0.037)	−45	8.73	0.008	0.178 (0.028)	0.121 (0.019)	−32	2.89	0.106	0.248 (0.035)	0.142 (0.032)	−43	5.19	0.035
Medial traverse	0.494 (0.044)	0.270 (0.003)	−45	18.3	<0.001	0.250 (0.028)	0.150 (0.022)	−40	8.32	0.010	0.243 (0.022)	0.149 (0.019)	−39	9.57	0.006
Central traverse	0.500 (0.041)	0.225 (0.032)	−55	26.6	<0.001	0.117 (0.009)	0.052 (0.006)	−55	26.6	<0.001	0.266 (0.022)	0.146 (0.019)	−45	16.1	0.001
Mean	0.470 (0.035)	0.256 (0.028)	−45	23.5	<0.001	0.212 (0.022)	0.128 (0.013)	−40	10.3	0.005	0.258 (0.016)	0.146 (0.022)	−43	16.8	0.001
BasoMedial Nucleus															
Mean	0.811 (0.66)	0.386 (0.041)	−52	31.2	<0.001	0.334 (0.028)	0.202 (0.025)	−40	11.6	0.003	0.458 (0.060)	0.243 (0.019)	−47	11.9	0.003

[1]Results are in mean values (standard error of mean). Cluster density indicates the number of SST-positive cells per mm^2. Grey shades indicate significant effects ($p < 0.05$).

Depress Anxiety. Author manuscript; available in PMC 2018 January 01.

Table 3

SST reduction per SST-positive cell in the amygdala.

	All					Large clusters					Small Clusters				
	Control[1]	**MDD[1]**	**%**	**F**	**p-value**	**Control[1]**	**MDD[1]**	**%**	**F**	**p-value**	**Control[1]**	**MDD[1]**	**%**	**F**	**p-value**
Lateral nucleus															
Lateral traverse	0.332 (0.041)	0.309 (0.041)	−7	0.14	0.711	0.393 (0.047)	0.358 (0.063)	−9	0.20	0.663	0.296 (0.041)	0.307 (0.035)	4	0.04	0.838
Medial traverse	0.359 (0.032)	0.355 (0.035)	−1	0.01	0.934	0.447 (0.047)	0.461 (0.044)	3	0.04	0.836	0.301 (0.032)	0.259 (0.022)	−14	1.20	0.287
Central traverse	0.385 (0.028)	0.333 (0.019)	−13	2.31	0.146	0.487 (0.028)	0.446 (0.032)	−8	0.84	0.370	0.318 (0.032)	0.282 (0.025)	−11	0.75	0.399
Mean	0.379 (0.025)	0.344 (0.022)	−9	1.03	0.324	0.480 (0.032)	0.426 (0.038)	−11	1.17	0.294	0.314 (0.025)	0.274 (0.016)	−13	1.87	0.189
BasoLateral nucleus															
Lateral traverse	0.424 (0.025)	0.437 (0.044)	3	0.06	0.807	0.586 (0.035)	0.509 (0.047)	−13	1.57	0.227	0.317 (0.025)	0.342 (0.019)	8	0.58	0.457
Medial traverse	0.457 (0.016)	0.396 (0.016)	−13	7.02	0.016	0.567 (0.028)	0.489 (0.032)	−14	3.52	0.077	0.338 (0.025)	0.296 (0.035)	−13	1.04	0.320
Central traverse	0.375 (0.028)	0.394 (0.035)	5	0.17	0.687	0.533 (0.003)	0.481 (0.044)	−8	0.42	0.524	0.271 (0.022)	0.299 (0.060)	10	0.20	0.663
Mean	0.426 (0.019)	0.406 (0.022)	−5	0.53	0.478	0.564 (0.028)	0.496 (0.032)	−12	2.67	0.120	0.314 (0.019)	0.309 (0.028)	−2	0.02	0.885
BasoMedial Nucleus															
Mean	0.495 (0.032)	0.373 (0.044)	−25	5.23	0.035	0.557 (0.035)	0.445 (0.032)	−20	5.27	0.034	0.338 (0.028)	0.229 (0.019)	−32	9.60	0.006

[1]Results are represented as mean values (standard error of mean). The amount of SST per SST-positive cell body is expressed in ratio of cell body covered by silver grains (See methods). Grey shades indicate significant effects ($p < 0.05$).